Chapter 5

Thermal Performance

The crucial parameter in designing npps is the produced in the core and its removal by the coolant. To that end, water coolant at 280 to 340 °C and heat flows from the fuel rods to the coolant. Since heat is generated inside the fuel rods and flows radially outward, the temperature gradients are established within the rods and it strongly affects the performance and properties of the materials.

High operating temperature lead to high thermal efficiency, but severe material degradation processes are accelerated with temperature. Temperature gradients in the fuel can cause stress and fuel cracking. In this section, we predict temperature gradient of fuel-cladding system, which is a key to control the performance of the npps.

5.1 Fission heat generation

Fission splits the uranium atom into two lower-mass isotopes (fission products) and release two to three energetic neutrons (average energy $\sim 2\,\mathrm{MeV}$) as well as other particles, such as α, β and neutrinos. The overall energy release in a single fission reaction is about 200 MeV and around 95% of which (190 MeV) is deposited in the fuel pellet. In thermal reactors, which is PWR (Pressurized Water Reactor), $\sim 2\,\mathrm{MeV}$ neutrons reduce their energy to the thermal energy $\sim 0.025\,\mathrm{eV}$ by the passage of the moderator (water).

In parallel with neutron-induced fission, uranium absorbs neutrons to from transuranic elements. The most important transuranic nuclide is Pu-239, which is formed by neutron absorption of U-238 followed by β decay. At the end of the fuel residence time in the reactor, up to one-third of the reactor energy is produced by plutonium fission. In reactor core of PWR, there are many heat sources:

- Fast fission of U-238
- Thermal fission of U-235
- Thermal fission of Pu-239
- etc.

In beginning of fuel element life, the fission rate is given by

$$\dot{F}(t) = q(t) N_{\mathrm{U}}(t) \sigma_{\mathrm{f}}^{\mathrm{U}-235} \phi_{\mathrm{th}}$$

where

- q is the enrichment of U-235, typically 0.02 to 0.05.
- Thermal neutron flux, ϕ_{th} is $\sim 2 \times 10^{13}\text{n/cm}^2\text{s}$
- The thermal fission cross section of U-235, $\sigma_{\text{f}}^{\text{U}-235}$ is $5.5\times10^{-22}\text{cm}^2$ or 550 barns.
- N_{U} is the density of UO_2 is $2.5 \times 10^{22}\text{atom/cm}^3$.

It gives the fission-rate density

$$\dot{F} = 0.8 \sim 1.3 \times 10^{13}\text{s}^{-1}\text{cm}^{-3}$$

which is equivalent to a *linear heat rate*(LHR) as high as 300 W/cm for a standard fuel rod.

5.2 Fuel burnup

There are three measures of burnup. The fission density (fissions per unit volume) given by

$$F = \int_0^t \dot{F}(t')dt'[\text{fission/m}^3]$$

The fissions per initial metal atom (FIMA):

$$\text{FIMA} = \frac{F}{N_{\text{U}}(0)}$$

bu is the number of megawatts days of thermal energy released by a fuel initially containing 1 kg of uranium. The 190 MeV released in each fission that is deposited in the fuel corresponds to 3.0×10^{-11}J. It can be converted to

$$1\text{bu} = 1\frac{\text{MWd}}{\text{kgU}} = 887\text{FIMA}$$

Usually, the average fuel discharge is about 50bu for PWR. The NRC (Nuclear Regulatory Commission) has established a burnup limit of 62.5bu.

5.3 Fission heat removal

The thermal design of a fuel element is constrained by various limits. The difference between a limiting condition and the actual state of the fuel is termed the *margin*. One of the important condition is fuel not have to be melt. The melting temperature of fuel is 3140 K or 2867 °C and that of Zr cladding is 2150 K and 1877 °C.

Large temperature gradients in the fuel should be avoided many issues; we do not cover it seriously in this class. These constrains dictate a fuel with high thermal conductivity. This is best achieved with metallic fuels, whose thermal conductivities are much higher than that of UO_2. However, metallic fuels exhibit serious dimensional instabilities under irradiation, while uranium dioxide is a remarkably stable matrix being able to undergo thermal cycling.

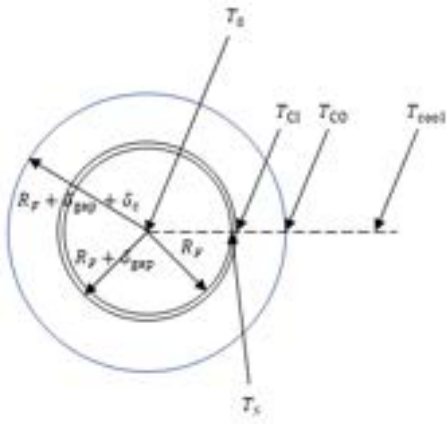

Figure 5.1: The heat transfer geometry in a nuclear fuel rod.

5.3.1 Heat conduction in the fuel

Ninety-five percent of fission energy is removed as heat from the fuel element by *conduction* in the geometry shown in Fig. 5.1. Heat is generated in the pellet and flows radially through the fuel, the pellet-cladding gap, and the cladding proper to reach the coolant. Because the axial temperature variation is relatively gradual and there is comparatively less azimuthal temperature variation, considering only *radial* heat flow is a good approximation. The steady-state heat conduction equation is

$$\frac{1}{r}\frac{d}{dr}\left(rk_{\mathrm{F}}\frac{dT(r)}{dr}\right)+Q(r)=0 \tag{5.1}$$

where T is the temperature, r is the radial position in the pellet, k_{F} is the fuel thermal conductivity, and $\overline{Q}$ is the volumetric heat generation rate given, assumed homogeneous for simplicity,

$$\overline{Q}=3.0\times10^{-11}\dot{F}$$

And LHR is usually approximated by

$$\mathrm{LHR}=\pi R_{\mathrm{F}}^2\overline{Q} \tag{5.2}$$

With boundary condition impose to Eq. 5.1,

$$T(R_{\mathrm{F}})=T_{\mathrm{S}} \qquad \left.\frac{dT(r)}{dr}\right|_{r=0}=0$$

Then,

$$T(r)-T_{\mathrm{S}}=\frac{\overline{Q}R_{\mathrm{F}}^2}{4k_{\mathrm{F}}}\left(1-\frac{r^2}{R_{\mathrm{F}}^2}\right)=\frac{\mathrm{LHR}}{4\pi k_{\mathrm{F}}}\left(1-\frac{r^2}{R_{\mathrm{F}}^2}\right) \tag{5.3}$$

or

$$\frac{T(r)-T_{\mathrm{S}}}{T_0-T_{\mathrm{S}}}=1-\frac{r^2}{R_{\mathrm{F}}^2} \tag{5.4}$$

where T_0 is the fuel centerline temperature. Thus a parabolic temperature profile is established whenever heat generation and fuel thermal conductivity are radially constant.

From Eq. 5.3,

$$T_0-T_{\mathrm{S}}=\frac{\mathrm{LHR}}{4\pi k_{\mathrm{F}}} \tag{5.5}$$

The equivalent calculations for plate is

$$T(x) - T_{\mathrm{S}} = \frac{\mathrm{LHR}}{2\pi k_{\mathrm{F}}}\left(1 - \frac{x^2}{t_{\mathrm{F}}^2}\right)$$

where t_{F} is the plate fuel thickness. For spherical fuel,

$$T(r) - T_{\mathrm{S}} = \frac{\mathrm{LHR}}{6\pi k_{\mathrm{F}}}\left(1 - \frac{r^2}{R_{\mathrm{F}}^2}\right)$$

where r is the radius of spherical fuel. The average fuel temperature is calculated using

$$\overline{T} = \frac{1}{\pi R_{\mathrm{F}}^2}\int_0^{R_{\mathrm{F}}} 2\pi r T(r) dr = 2\int_0^1 \eta T(\eta) d\eta \tag{5.6}$$

where

$$\eta = \frac{r}{R_{\mathrm{F}}}$$

Plug Eq. 5.4 into Eq. 5.6, we have

$$\overline{T} = \frac{T_0 + T_{\mathrm{S}}}{2}$$

5.3.2 Heat transfer resistance beyond the fuel

Heat transfer through the gap is characterized by a conductance, $h_{\mathrm{gap}}(\mathrm{W/m^2 \cdot K})$. If the gap is open,

$$h_{\mathrm{gap}} = \frac{k_{\mathrm{gap}}}{\delta_{\mathrm{gap}}} \tag{5.7}$$

where δ_{gap} is the gap thickness and k_{gap} is the thermal conductivity of the gas in the gap and k_{gap} is the thermal conductivity of the gas in the gap. In as-fabricated fuel rods, the gap is filled with helium at ~ 10 atm pressure. The reason for initial pressurization is to avoid drastic thermal-conductivity reduction as fission gases such as xenon and krypton are released from the fuel. The thermal conductivities of these gases are

$$k_{\mathrm{gas}} = A \times 10^{-4} T^{0.79} \mathrm{W\,m^{-1}\,K^{-1}} \tag{5.8}$$

where $A = 16$ for He and $A = 0.7$ for Xe. A simple mixing rule yields

$$k_{\mathrm{gap}} = k_{\mathrm{He}}^{1-y} k_{\mathrm{Xe}}^{y}$$

where y is the fraction of Xe in the gas mixture.

Since the gap thickness is much less than the fuel radius, the heat flux through the gap is

$$q = \frac{\mathrm{LHR}}{2\pi R_{\mathrm{F}}} = h_{\mathrm{gap}}(T_{\mathrm{S}} - T_{\mathrm{CI}})$$

or

$$T_{\mathrm{S}} - T_{\mathrm{CI}} = \frac{\mathrm{LHR}}{2\pi R_{\mathrm{F}} h_{\mathrm{gap}}} \tag{5.9}$$

where T_{CI} is the cladding inner-surface temperature.

The next resistance in series in the cladding, for which an analysis similar to that for the gap yields

$$T_{\mathrm{CI}} - T_{\mathrm{CO}} = \frac{\mathrm{LHR}}{2\pi k_{\mathrm{C}}}\left[\ln\left(\frac{R_{\mathrm{F}} + \delta_{\mathrm{C}}}{R_{\mathrm{F}}}\right)\right] \tag{5.10}$$

Because the cladding is tabular, Eq. 5.10 can be approximated when $\delta_C \ll R_F$,

$$T_{CI} - T_{CO} = \frac{\text{LHR}}{2\pi R_F k_C/\delta_C}$$

T_{CO} is the cladding outer-surface temperature.

Heat transfer from the cladding outer diameter to the coolant occurs by convection:

$$T_{CO} - T_{cool} = \frac{\text{LHR}}{2\pi R_F h_{cool}} \tag{5.11}$$

Adding Eqs. 5.9, 5.10 and 5.11,

$$T_S - T_{cool} = \frac{\text{LHR}}{2\pi R_F h} \tag{5.12}$$

where

$$\frac{1}{h} = \frac{1}{h_{gap}} + \frac{\delta_C}{k_C} + \frac{1}{h_{cool}}$$

With the typical numbers,

$$T_{cool} = 580\,\text{K} \qquad \text{LHR} = 20\,000\,\text{W/m}$$

$$h_{cool} = 26\,500\,\text{W/m}^2\cdot\text{K} \qquad k_{He} = 0.25\,\text{W/m}\cdot\text{K}$$

The pellet radius and cladding thickness are

$$R_F = 5\times10^{-3}\text{m} \qquad \delta_C = 6\times10^{-4}\text{m}$$

The gap width is

$$\delta_{gap} = 3\times10^{-5}\text{m}$$

From Eq. 5.11,

$$T_{CO} = 601\,\text{K}$$

From Eq. 5.10,

$$T_{CI} = 631\,\text{K}$$

When He is filled in the gap, from Eq. 5.8,

$$k_{gas} = 0.25\,\text{W/m}\cdot\text{K}$$

From Eq. 5.7,

$$h_{gap} = 7050\,\text{W/m}^2\cdot\text{K}$$

From Eq. 5.9,

$$T_S = 705\,\text{K}$$

From Eq. 5.5,

$$T_0 = 1236\,\text{K} \tag{5.13}$$

As burn up progresses, the porosity of fuel increases. Let's assume the porosity is 5% after some degree of burn up. The density of UO_2 is $10.98\,\text{kg/m}^3$ and length of fuel stack is 300 cm and plenum length is 20 cm. The average molecular weight of fuel is assumed by 270. Then

$$\text{Moles } UO_2 = \frac{\pi\times0.5^2\times300\times0.95\times10.98}{270} = 9.1$$

The gas space in rod is when the gap is 80 μm,

$$\pi \times 0.5^2 \times 20 + 2\pi \times 0.5 \times 0.008 \times 300 = 15.7 + 7.5 = 23.2 \times 10^{-7}\,\mathrm{m}^3$$

Initially, the moles of He is at $T = 373\,\mathrm{K}$

$$\text{Moles He} = \frac{10 \times 23.2}{82 \times 373} = 7.6 \times 10^{-3}$$

assume that it follows state equation for ideal gas. When Xe fission yield is 0.25, and burnup is 3%, then amount of Xe produced is

$$9.1 \times 0.03 \times 0.25 = 0.068\,\mathrm{mol}$$

Assume that 6% of fission gas is released, then

$$0.068 \times 0.06 = 4.1 \times 10^{-3}\mathrm{mol}$$

of Xe is released, that the fraction of Xe for the gas in the gap is

$$\frac{4.1}{7.6 + 4.1} = 0.35$$

Since

$$k_{\mathrm{He}} = 0.25 \qquad k_{\mathrm{Xe}} = 6.9 \times 10^{-3}$$

we have

$$k_{\mathrm{gap}} = (0.25)^{0.65}(6.9 \times 10^{-3})^{0.35} = 7.22 \times 10^{-2}$$

Then

$$h_{\mathrm{gap}} = 241\,\mathrm{W/m^2 \cdot K}$$

Then we have

$$T_{\mathrm{S}} - T_{\mathrm{CI}} = 188\,\mathrm{K}$$

The Xe in the gap increases ΔT_{gap} by 100 K, which would make the

$$T_0 = 1424\,\mathrm{K}$$

If during fabrication of the fuel rod the gap had contained 1 atm He instead of 10 atm, the gap gas composition would have been 84% Xe. k_{gap} would have been reduced to $0.0125\,\mathrm{W\,m^{-1}\,K^{-1}}$ and ΔT_{gap} would have been an unacceptable 1524 K.

5.4 Gap closure on initial heatup

There are two causes of fuel-cladding gap closure at startup: thermal expansion and fuel cracking. Here we deal in detail only with the first.

The change in gap width upon fuel and cladding expansion is given by

$$\Delta\delta_{\mathrm{gap}} = \delta_{\mathrm{gap}} - \delta^{\mathrm{o}}_{\mathrm{gap}} = \Delta\overline{R}_{\mathrm{C}} - \Delta R_{\mathrm{F}}$$

The superscript o indicates as-fabricated value. $\Delta\overline{R}_{\mathrm{C}}$ is the change in mean cladding radius, and ΔR_{F} is the change in the fuel-pellet radius, both as a result of the temperature increase on startup in the reactor. The radial strain of the fuel in a parabolic temperature profile is given by

$$\frac{\Delta R_{\mathrm{F}}}{R_{\mathrm{F}}} = \alpha_{\mathrm{F}}(\overline{T}_{\mathrm{F}} - T_{\mathrm{fab}})$$

	1	2	3	4	5	6
Initial T_S	680	690	700	710	720	715
$T_0 = T_S + \mathrm{LHR}/(4\pi k_F)$	1078	1088	1098	1108	1118	1113
$\overline{T}_F = 1/2(T_s + T_0)$	879	889	899	909	919	914
$\overline{R}_F = \overline{R}_F^\circ[1 + \alpha_F(\overline{T}_F - T_{fab})]$	0.5036	0.5037	0.5038	0.5039	0.5040	0.5040
$\delta_{gap} = \overline{R}_c - \delta_C/2 - R_F$	54	53	52	51	50	50
$h_{gap} = k_{He}/\delta_{gap}$	0.469	0.475	0.482	0.489	0.496	0.493
$T_S = T_{CI} + \frac{\mathrm{LHR}}{2\pi \overline{R}_F^\circ h_{gap}}$	720	718	717	716	714	715

Table 5.1: Trial-and-error solution

where $\overline{T}_F$ is the average fuel rod temperature. T_{fab} is the fuel fabrication temperature, and α_F is the coefficient of thermal expansion of UO_2. The corresponding increase for the cladding is approximately equal to

$$\frac{\Delta R_C}{R_C} = \alpha_C(\overline{T}_C - T_{fab})$$

An approximation to the change in gap width upon heating is given by

$$\Delta\delta_{gap} = \delta_{gap}^{hot} - \delta_{gap}^{fab} = \overline{R}_C^\circ \alpha_C(\overline{T}_C - T_{fab}) - \overline{R}_F^\circ \alpha_F(\overline{T}_F - T_{fab}) \tag{5.14}$$

The uncertainty in Eq. 5.14 is the mean fuel temperature, $\overline{T}_F$, which is a function of the gap thickness, which is the unknown. When

$$\mathrm{LHR} = 15\,000\,\mathrm{W\,m^{-1}} \qquad \delta_{gap}^\circ = 80\,\mu\mathrm{m} \qquad T_{fab} = 373\,\mathrm{K}$$

Since

$$T_{CO} = 601\,\mathrm{K} \qquad T_{CI} = 631\,\mathrm{K}$$

Then

$$\overline{T}_C = 615\,\mathrm{K}$$

If

$$\delta_C = 0.1\,\mathrm{cm}$$

then at $T = T_{fab} = 373\,\mathrm{K}$,

$$\overline{R}_C^\circ = 0.5 + 0.008 + \frac{1}{2} \times 0.1 = 0.558\,\mathrm{cm}$$

And we assume that $T = T_S = 678\,\mathrm{K}$

$$\overline{R}_C = \overline{R}_C^\circ[1 + \alpha_C(\overline{T}_C - T_{fab})] = 0.559\,\mathrm{cm}$$

To solve the solution, we can have the iteration approach. Accounting for thermal expansion of fuel and cladding (and for the different specification of the size of the as-fabricated gap) increases the calculated at-power gap thickness to $50\,\mu$m. This results in a larger temperature drop over the gap and an increase in the fuel-centerline temperature from 1076 K to 1113 K. The very significant effect of the $20\,\mu$m increase in gap thickness is due to the poor thermal conductivity of helium.

Using the vale of 877 K and the as-fabricated gap thickness of $80\,\mu$m, the hot-gap size from Eq. 5.14 is $54\,\mu$m. This is only $4\,\mu$m larger than the value calculated from former context. Unless high accuracy is required, the approach we used is good enough.

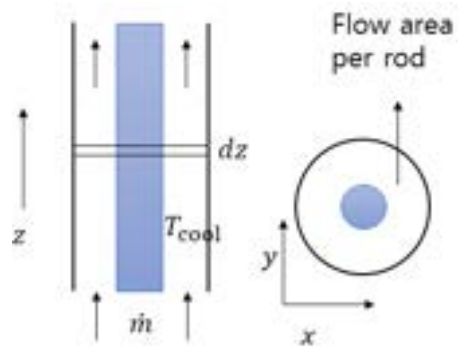

Figure 5.2: Upflow of coolant per fuel rod.

The tangential stress in the fuel pellet subject to a radially-constant heat generation rate is

$$\sigma_\theta = -\frac{\alpha_{\mathrm{F}} E_{\mathrm{F}}(\mathrm{LHR})}{16\pi(1-\nu_{\mathrm{F}})k_{\mathrm{F}}}\left(1-3\frac{r^2}{R_{\mathrm{F}}^2}\right)$$

E_{F} is the elastic constant of UO_2 and ν_{F}, its Poisson ratio. The outer 40% of the pallet is under tensile stress(azimuthal) that, for usual LHRs, exceeds the fracture stress. A typical cracking pattern is shown in Fig. 1.11.

5.5 Axial Temperature Profile

The calculations in previous section were performed for radial transfer of heat. Because of temperature differences along the length of the fuel rod, heat is also transferred in the axial direction. The axial variation of the linear heat rate can be written as

$$\mathrm{LHR}\left(\frac{z}{Z_0}\right) = \mathrm{LHR}^\circ \cos\left[\frac{\pi}{2\gamma}\left(\frac{z}{Z_0}-1\right)\right] = \mathrm{LHR}^\circ f\left(\frac{z}{Z_0}\right)$$

$$f(x) = \cos\left[\frac{\pi}{2\gamma}(x-1)\right]$$

where z is the axial distance, LHR° is the centerline linear heat rate ($z/Z_0 = 1$), and $\gamma = (Z_{\mathrm{ex}} + Z_0)/Z_0$ represents the ratio of the extrapolation distance of the neutron flux to the fuel-rod half-height. A typical value is $\gamma = 1.3$. Angles are expressed in radians.

Because of the above variation of the LHR and the increasing temperature of the coolant as it passes through the core, the fuel supports an axial temperature profile. In Fig.5.2, the rod and associated coolant flow in the z direction, the energy balance of the circular slice dz is

$$\dot{m}C_{\mathrm{PW}}\frac{dT_{\mathrm{cool}}}{dz} = \mathrm{LHR}\left(\frac{z}{Z_0}\right)$$

Integrating from the core entry ($z = 0$) to height z,

$$\dot{m}C_{\mathrm{PW}}(T_{\mathrm{cool}} - T_{\mathrm{cool}}^{\mathrm{in}}) = Z_0\int_0^{z/Z_0}\mathrm{LHR}\left(\frac{z}{Z_0}\right)d\left(\frac{z}{Z_0}\right)$$

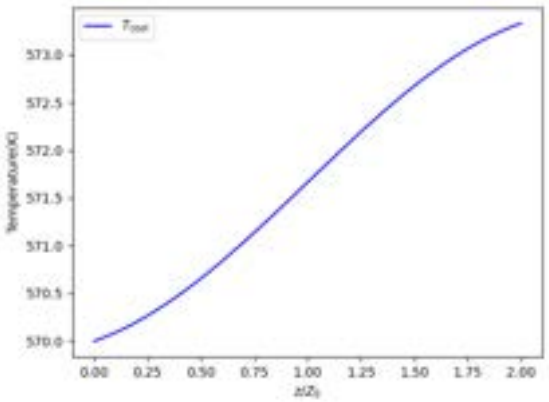

Figure 5.3: Axial temperature distributions

where $\dot{m}$ is the mass flow rate per fuel rod ($\mathrm{kg\,s^{-1}\,rod^{-1}}$), C_{PW} is the coolant specific heat ($\mathrm{J\,kg^{-1}\,K^{-1}}$) and $T_{\mathrm{cool}}^{\mathrm{in}}$ is the inlet coolant temperature. Then

$$\dot{m}C_{\mathrm{PW}}\left(T_{\mathrm{cool}} - T_{\mathrm{cool}}^{\mathrm{in}}\right) = Z_0 \times \mathrm{LHR}^{\circ} \int_0^{z/Z_0} f\left(\frac{z}{Z_0}\right) d\left(\frac{z}{Z_0}\right)$$

proceed to

$$T_{\mathrm{cool}} - T_{\mathrm{cool}}^{\mathrm{in}} = \frac{1}{1.2} \frac{Z_0 \times \mathrm{LHR}^{\circ}}{\dot{m}C_{\mathrm{PW}}} \left\{ \sin\left(1.2\right) + \sin\left[1.2\left(\frac{z}{Z_0} - 1\right)\right] \right\}$$

When

$$\frac{z}{Z_0} = 1 \qquad \dot{m} = 0.25\,\mathrm{kg\,s^{-1}\,rod^{-1}} \qquad Z_0 = 0.15\,\mathrm{m}$$

$$\mathrm{LHR}^{\circ} = 15\,000\,\mathrm{W\,m^{-1}} \qquad C_{\mathrm{PW}} = 4200\,\mathrm{J\,kg^{-1}\,K^{-1}} \qquad T_{\mathrm{cool}}^{\mathrm{in}} = 570\,\mathrm{K}$$

As expected, the highest temperature occurs at the core outlet ($z/Z_0 = 2$). However, the fuel centerline temperature reaches its maximum above the core midplane in Fig. 5.3.

5.6 Thermal Conductivity

The heat conduction equations derived above apply only when the thermal conductivity is constant, whereas it actually depends on temperature, chemistry and fuel microstructure. The thermal conductivity of the fuel depends on temperature, composition and burnup. Knowledge of the thermal conductivity of the fuel, gap, and cladding is essential to determining the temperature distribution and transient thermal response of the fuel rod. The thermal conductivity of the fuel also determines the amount of stored heat in the fuel, which is a consequence of the large gradients that have to be established to sustain heat flow at steady state.

The thermal conductivity of pure UO_2, UO_{2+x}, UO_2 with cation impurities (e.g., $(U,Pu)O_2$) and irradiated UO_2.

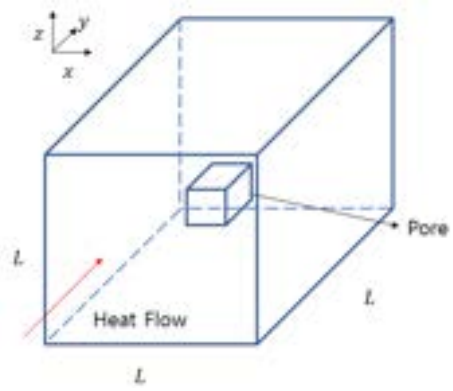

Figure 5.4: Geometry for analysis of effect of pores on thermal conductivity

5.6.1 Thermal conductivity in porous oxide

When uranium dioxide is fabricated into pellets, sintering conditions can be controlled so that the pores initially present are partially eliminated, resulting in solid with 94% to 96% of the theoretical density of UO_2 ($10.95\,g/cm^3$). The pores provide free space to accommodate fission gases, thus reducing swelling. However, porosity diminishes the thermal conductivity of the pellet. During irradiation, additional porosity develops in the form of fission-gas-filled bubbles.

Consider a homogeneous distribution of cube-shaped pores in which a "unit cell" consists of the pore and its associated in Fig. 5.4. Two pathways exist for heat flow along y direction: through the "pore tube" or through the solid surrounding the pore tube. On the latter route, the thermal conductivity is that of fully dense UO_2. Heat flow through the pore tube is governed by the thermal conductivity of a composite of void space and solid. The pore tube and the surrounding solid are parallel thermal resistances, so the effective thermal conductivity of the unit cell (i.e. of the fuel) is

$$k_F = (1-f)k_{ox} + fk_{\text{pore tube}}$$

where f is the fraction of the cross-sectional area perpendicular to heat flow occupied by the pore tube and k_{ox} is the thermal conductivity of fully dense UO_2. $k_{\text{pore tube}}$ represents the series thermal resistances of oxide and the pore, so

$$\frac{1}{k_{\text{pore tube}}} = \frac{g}{k_{\text{pore}}} + \frac{1-g}{k_{ox}}$$

where g is the fraction of the pore tube occupied by the pore. Eliminating $k_{\text{pore tube}}$ between these two equations yields

$$\frac{k_F}{k_{ox}} = \frac{1+(\xi-1)(1-f)g}{1+(\xi-1)g}$$

The right term is a correction factor on the thermal conductivity of 100%-dense UO_2. It depends on the geometry of the pore/solid unit cell (via f and g) and the ratio of the thermal conductivities of the oxide and the gas in the pore $\xi = k_{ox}/k_{\text{pore}}$. If either f or g is zero, the correction factor is unity. If $\xi = \infty$, the correction factor is $1-f$, or no heat flows through the pore tube.

The porosity of the fuel in Eq. 10.35 of [1] is

$$\mathcal{P} = fg$$

and if the pore is a cube,

$$f = \mathcal{P}^{2/3} \qquad \text{and} \qquad g = \mathcal{P}^{1/3}$$

In terms of the porosity, we have

$$\frac{k_{\mathrm{F}}}{k_{\mathrm{ox}}} = \frac{1 + (\xi - 1)\big(1 - \mathcal{P}^{2/3}\big)\mathcal{P}^{1/3}}{1 + (\xi - 1)\mathcal{P}^{1/3}}$$

When $(\xi - 1)\mathcal{P}^{1/3} \gg 1$,

$$\frac{k_{\mathrm{F}}}{k_{\mathrm{ox}}} = 1 - \mathcal{P}^{2/3}$$

When

- for as-fabricated fuel, $\mathcal{P} = 0.05$,
- the pores are filled with 65% helium and 35% xenon - $k_{\mathrm{pore}} \simeq 8 \times 10^{-2} \mathrm{W\,m^{-1}}$
- UO_2 thermal conductivity is $k_{\mathrm{ox}} \simeq 3\,\mathrm{W\,m^{-1}\,K^{-1}}$, so $\xi = 36$.

then we have

$$\frac{k_{\mathrm{F}}}{k_{\mathrm{ox}}} = 0.87$$

That is, a 13% reduction in effective thermal conductivity relative to that of the solid UO_2.

5.6.2 Thermal conductivity variation with temperature

The integration of Eq. 5.1 was performed assuming the thermal conductivity to be independent of the radial position r. In fact, the thermal conductivity of UO_2 varies significantly with temperature, which in turn varies markedly with radial position.

Rather than a constant, a typical temperature-dependent thermal conductivity is

$$k_{\mathrm{ox}} = \frac{1}{A + BT}\big(\mathrm{W\,m^{-1}\,K^{-1}}\big)$$

where

$$A = 3.8{+}200{\times}\mathrm{FIMA{\cdot}cm \cdot K/W} \qquad B = 2.17{\times}10^{-4}\mathrm{m\,W^{-1}} = 0.0217{\times}10^{-4}\mathrm{cm\,W^{-1}}$$

which is a well-known empirical fit of thermal conductivity data, is referred to as the Halden equation after Norwegian laboratory where these data were generated. Neglecting porosity $\big(k_{\mathrm{F}} \simeq k_{\mathrm{ox}}\big)$, the temperatures at the fuel centerline and fuel surface are related by

$$\frac{1}{B} \ln\left(\frac{A + BT_0}{A + BT_{\mathrm{S}}}\right) = \frac{\mathrm{LHR}}{4\pi}$$

Numerous correlations of k_{ox} have been prepared by Baron[2], which, in addition to temperature and porosity dependences, include the effects of plutonium and gadolinium.

To account for the dependence of thermal conductivity on temperature, stoichiometry, and plutonium content, the heat conduction equation would need to be solved with k_{ox} as a function of these variables.

For example, assuming $T_{\mathrm{S}} = 714\,\mathrm{K}$, the centerline temperature can be estimated by

$$\exp\left(\frac{B \times \mathrm{LHR}}{4\pi}\right) = \exp\left(\frac{0.0217 \times 200}{4\pi}\right) = 1.41$$

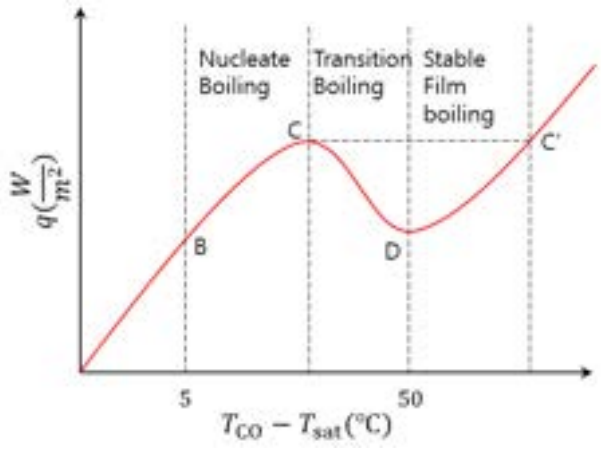

Figure 5.5: Schematic of boiling curve in an LWR.

$$A + BT_S = 3.8 + 0.0217 \times 714 = 19.3 \qquad T_0 = \frac{19.3 \times 1.41 - 3.8}{0.0217} = 1081\,\mathrm{K}$$

which differs T_0 from Eq. 5.13. This occurs because the thermal conductivity of UO_2 increases with T and the constant $k_F = 0.03\,\mathrm{W\,cm^{-1}\,K^{-1}}$ is only a very rough average.

5.7 Thermal Margins and Operating Limits

A nuclear reactor is different from conventional power plants in one important way: The central safety tenet in nuclear power plant operation is avoidance of fuel damage and attendant release of fission products. To avoid fuel damage, the operational constraints are imposed on maximum fuel centerline temperature. Because the neutron flux and coolant temperature vary axially and radially through the core, so do the fuel-rod temperatures.

5.7.1 Critical heat flux

As the outer surface temperature of a heated fuel rod immersed in a constant temperature liquid increases, the mode of heat transfer changes. The typical *boiling curve* of LWR is described in Fig. 5.5.

1. When $T_{CO} - T_{sat} < 5\,^\circ\mathrm{C}$, a flux q is driven by the temperature difference between outer surface of cladding and bulk coolant,

$$q = h\big(T_{CO} - T_{sat}\big)$$

Using thermalhydraulic properties of the coolant, we have

$$\frac{hd_{eq}}{k_{cool}} = 0.023\mathrm{Re}^{0.8}\mathrm{Pr}^{0.4}$$

where d_{eq} is the equivalent diameter of the flow channel, k_{cool} is the thermal conductivity of the coolant, and Re and Pr are the Reynolds and Prandtl numbers.

One of the main concerns for fuel rods is that the linear heat flux becomes so high that *dryout* occurs. Fig. 5.5 shows the rise of the outer cladding temperature T_{CO} as the heat flux q from the fuel to the coolant increase. At point B, the onset of *nucleate boiling* provides greater mixing and heat transfer to the coolant.

Nucleate boiling begins at point B, a empirical correlation applicable to PWR conditions for this scheme is

$$q\big(\mathrm{W/m^2}\big) = 6\big(T_{\mathrm{CO}} - T_{\mathrm{sat}}\big)^4$$

The heat transfer through one-phase, liquid water.

2. The regime between B to C, the mechanism of heat transfer from the cladding outer surface to the bulk coolant is more complex than a one-phase heat transfer. As the temperature of the cladding outer diameter increases beyond point B, so too does the bubble concentration in the fluid near the wall. At a critical point (C), the bubbles coalesce and a continuous film of steam is formed. Point C is known as the *critical heat flux* (CHF). In PWRs, this point is identified as the *departure from nucleate boiling*(DNB). At this point, nuclear boiling turns into the very-much-less-efficient *film boiling*.

3. Beyond point C, the rod is blanketed by steam and the heat flux is severely decreased as the heat transfer coefficient from cladding to steam is much lower than that of cladding to water. In Fig. 5.5,

$$T_{\mathrm{CO}} - T_{\mathrm{cool}} = \big(T_{\mathrm{CO}} - T_{\mathrm{sat}}\big) + \big(T_{\mathrm{sat}} - T_{\mathrm{cool}}\big)$$

this is because the boiling curves depend upon the *difference* between the wall temperature and the saturation temperature, not the bulk coolant temperature. In a PWR, $T_{\mathrm{sat}} = 615\,\mathrm{K}$. A typical cladding OD temperature is $T_{\mathrm{CO}} \simeq 633\,\mathrm{K}$.

4. Above point C, the bubble nucleation rate becomes high enough that a continuous vapor film forms at the surface. In this region the heat transfer becomes very unstable and the temperature of the wall can suddenly change to one in the film-boiling regime.

The departure from nucleate boiling ratio (DNBR) is the ratio of the heat flux that causes dryout (CHF) to the actual heat flux. The DNBR scales with the incidence of fuel damage when these margins are obtained by calculations. In an operating nuclear power plant, the DNBR for the hottest channel is larger than 1.15 to 1.3, or a margin of 15% to 30%. As shown in Fig. 5.6, the hottest channel the location where the heat flux most closely approached the critical heat flux. When the critical heat flux is reached, the wall temperature increases precipitously, typically above 1100 K, and cladding failure is certain. To avoid reaching the critical heat flux, *thermal margin* are established. When that happens the liquid can only contact the cladding when the temperature is cooled down to point D in Fig. 5.5.

The mechanism above is prevalent in PWRs, in which a majority of the liquid phase is present where bubbles are generated. A *dryout* condition can then occur as a combination of droplet entrainment and evaporation takes place, at which point the flow becomes vapor with entrained droplets. The heat transfer then decreases abruptly, and a *critical heat flux* condition is again reached, this time by a dryout mechanism.

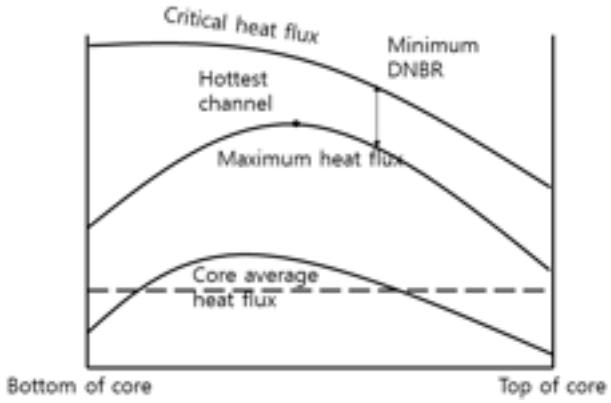

Figure 5.6: Departure from nucleate boiling limits.

5.7.2 Pellet-cladding mechanical interaction

Early reports of fuel failures by *pellet-cladding mechanical interaction*(PCMI) first appeared in the 1960s. If the linear heat rate is suddenly increased, the pellet-cladding gap closes and the fuel mechanically loads the cladding. If the resulting tensile stress in the cladding is high enough, failure can occur. This frequently occurs in fuel rods adjacent to a recently withdrawn control rod, which causes a sudden LHR increase. The PCMI mechanism is exacerbated when the fuel is cracked or when there is missing chip on the fuel surface, which tends to localize the deformation in the cladding. With longer exposure, the cladding becomes increasingly brittle, so that failure occurs at a smaller imposed strain.

Bibliography

[1] *Nuclear Heat Transport.*, El-Wakil, Mohamed Mohamed, 1970

[2] *Fuel thermal conductivity: a review of the modelling available for UO2,(U-Gd) O2 and MOX fuel*, B. Daniel, 1998